Time-frequency representations based detector of chaos in oscillatory circuits

Vesna Rubežić, Igor Djurović, Miloš Daković

Abstract— **Detection of chaotic states in the nonlinear chaotic Chua's oscillatory circuit has been considered. A new approach, based on the concentration measure of the time-frequency (TF) representation, is proposed for determination of the current circuit state. Parameters of the proposed algorithm are studied in details. The algorithm is applied in the case of moderate noisy signal, as well as for breaking a chaotic communication scheme.**

I. Introduction

Under the specific conditions, various nonlinear systems exhibit chaotic dynamic behavior (chaotic nonlinear circuits [1],[2], chaotic secure communication schemes [3],[4], chaotic watermarking systems [5], and various kinds of biomedical, mechanical, economical systems [6]-[8]). By varying their parameters, these systems could pass through the various types of bifurcations and steady states (equilibrium point, periodic, quasi-periodic, chaotic states). Chaotic systems are the nonlinear ones that are characterized by sensitive dependence on initial conditions. Common theoretical indication of chaos are Lyapunov coefficients. Namely, positive Lyapunov coefficients indicate exponential divergence of nearby system states. However, Lyapunov coefficients are not practically applicable since their evaluation requires very long signal sequence (theoretical of infinite length). In addition, Lyapunov coefficients are very sensitive to noise influence [9]-[13] and there are systems whose Lyapunov exponents are either not defined or difficult or impossible to calculate [14]-[16]. These drawbacks force the recent advance in development of reliable chaos detection measures, some of them analyzed in [9]. Detection of nonlinear behavior in the system is employed in group of chaos detection systems [9]-[11]. However, nonlinear dynamic is required but not sufficient condition for chaotic behavior. Some other techniques are based on pattern recognition of chaotic attractors [17], [18]. The main drawback of these techniques is calculation complexity. Details of currently used chaos detection algorithms and measures can be found in [9] and references therein.

In this paper we study chaotic oscillatory circuits as an important group of chaotic systems. Note that there are specially designed chaotic oscillators like, for example, Chua's circuit [19]. Also, the chaotic dynamics can be observed in other oscillatory circuits due to nonlinearities introduced by imperfection of fabrication. In periodic regime these circuits produce signals that can be represented as a sum of several sinusoidal components, i.e., as a sum of Dirac pulses in spectral domain. However, in chaotic regime numerous additional components in spectral domain can be observed. Then, information on the circuit state can be extracted from the signal spectra by using a properly designed measure that produces different results for periodic and chaotic regimes. Details related to the spectral analysis of signals produced by the chaotic nonlinear oscillators can be found in [19]. In order to be able to track time-varying circuit state, we employ the time-frequency (TF) representations as a generalization of the Fourier transform (FT) concept. An excellent overview of the TF methods and application including study of concentration measures can be found in [20]. Note that the TF signal analysis has already been used for study of the chaotic signals and systems in [21].

An algorithm for chaos detection in nonlinear oscillators proposed in this paper is based on the short-time Fourier transform (STFT), as the simplest TF representation (running window FT realization), and its energetic ver-

Signal Processing, Vol.86, No.9, Sep. 2006.

sion called spectrogram. A specific concentration measure has been proposed in order to be able to distinguish between chaotic and periodic regimes. State of the system is estimated without apriory knowledge on the structure and parameters of the oscillator. However, simulation examples in this paper are performed for the Chua's oscillatory circuit. Theoretical knowledge of its behavior is wide, since this circuit is the first one considered in science. Then, it was the simplest way to compare obtained results with the related theory. The proposed algorithm has three important favorable properties: evaluation of the measure requires short interval (window width); reasonable calculation complexity; robustness to moderate noise amount. The proposed technique is applied for breaking "secure" chaotic communications between transmitter and receiver.

The paper is organized as follows. In Section II, theoretical overview of the Chua's oscillatory circuit and spectral analysis of related signals is given. TF representations used for design of the chaotic state detector are also reviewed in this section. The proposed detector based on concentration measure of TF representation is introduced in Section III as a chaotic circuit state detector. Detailed numerical analysis is given in Section IV for three routes to chaos, as well as for noisy chaotic sequences. In order to generalize application of our detector, chaos detection in the Rossler and logistic map chaotic systems is considered. Also, it has been shown that "secure" chaotic communications could be broken by proper threshold selection in the proposed detector, Section V. Concluding comments are given in Section VI.

II. Theoretical review

A. Chua's circuit

Consider the Chua's circuit shown in Fig.1a, with its state equations given as:

$$\frac{dv_1}{dt} = \frac{1}{C_1}\left[G\left(v_2 - v_1\right) - f\left(v_1\right)\right]$$

$$\frac{dv_2}{dt} = \frac{1}{C_2}\left[G\left(v_1 - v_2\right) + i_3\right]$$

$$\frac{di_3}{dt} = \frac{1}{L}\left(-v_2 - R_0 i_3\right) \tag{1}$$

where $G = 1/R$ and $f\left(v_1\right)$ is the piece-wise linear $v - i$ characteristic of the Chua's diode (Fig.1b), given by

$$f\left(v_R\right) = G_b v_R + \frac{1}{2}\left(G_a - G_b\right)$$

$$\times\left(\left|v_R + E\right| - \left|v_R - E\right|\right) \tag{2}$$

where E is the breakpoint voltage of Chua's diode. Note that all state variables are functions of time $v_1 \equiv v_1(t)$, $v_2 \equiv v_2(t)$, $i_3 \equiv i_3(t)$. Hereafter, we drop this dependence from notation for the sake of brevity. In order to perform approximative spectral analysis, constant circuit parameters are assumed [19]. However, in various routes to chaos they can vary in time.

Circuit behavior in the linear regions of function $f(v_1)$ can be described by the eigenvalues of

$$\mathbf{J}_i = \begin{bmatrix} a_i & G/C_1 & 0 \\ G/C_2 & -G/C_2 & 1/C_2 \\ 0 & -1/L & -R_0/L \end{bmatrix} \tag{3}$$

where $i = 1, 2, 3$, specifies the linear parts of the function $f(v_1)$, $a_1 = a_3 = -\left(G + G_b\right)/C_1$ and $a_2 = -\left(G + G_a\right)/C_1$. Characteristic polynomial of $\mathbf{J}_i$ has three roots: γ_i that corresponds to the direct current (DC) component of the form $c_{i1}\exp(\gamma_i t)$, and a complex-conjugate pair $\sigma_i \pm j\omega_i$ that corresponds to the damped sinusoidal components $c_{i2}\exp(\sigma_i t)\exp(j\omega_i t)$. This is in accordance with [19] where approximative spectral analysis of chaotic oscillatory circuits has been considered. It has been shown that in periodic regime, signals produced by this circuit have several periodic components while in chaotic regimes they have broadband power spectrum with numerous additional components and noise-like structures. Then, we can conclude that detection of chaos in these circuits can be performed in spectral domain by designing a measure that can distinguish between periodic (with several sinusoidal components) and chaos (with broadband signal with numerous components) regimes.

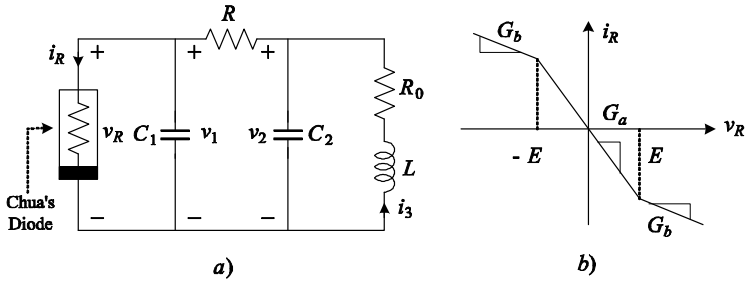

Fig. 1. (a) Chua's circuit; (b) nonlinear v-i characteristic of Chua's diode.

B. Time-frequency representations

Situation where some of circuit parameters vary in time and its values (current and past) determine circuit state is of our particular interest. Spectral content of signals produced with varying parameters in the circuit is time-varying (frequency of sinusoidal components vary, some components and noise like structures could appear or disappear in a signal). In the case of signals with time-varying contents it is required to design a representation that will give information on both temporal and spectral (frequency) signal behavior. The TF representations are used for this purpose.

The Fourier transform (FT) is a classical spectral analysis tool defined as:

$$X(f) = \int_{-\infty}^{\infty} x(t)e^{-j2\pi ft}dt. \tag{4}$$

Squared magnitude of the FT, $|X(f)|^2$, is called periodogram and it is used for approximative spectral analysis of signals produced by chaotic oscillatory circuits in [19].

The simplest TF representation is the STFT representing the FT calculated for signal windowed in the neighborhood of a considered instant:

$$STFT(t,f) = \int_{-\infty}^{\infty} x(t+\tau)w(\tau)e^{-j2\pi f\tau}d\tau, \tag{5}$$

where $x(t)$ is the signal of interest (here it means voltage or current), while $w(\tau)$ is (running or sliding) window function. The STFT has several important favorable properties including:

1. Linearity. The STFT of weighted sum of signals $z(t) = ax(t)+by(t)$ is equal to weighted sum of signals' STFTs: $STFT_z(t,f) = aSTFT_x(t,f) + bSTFT_y(t,f)$.

2. Time-frequency shift. For time and frequency shifted signal $y(t) = x(t-t_0)e^{j2\pi f_0 t}$ the STFT is shifted in the TF plane:

$$STFT_y(t,f) = STFT_x(t-t_0, f-f_0)e^{j2\pi f_0 t}. \tag{6}$$

However, the STFT is complex valued, and its energetic version called spectrogram: $SPEC(t,f) = |STFT_x(t,f)|^2$ is used in practice [22]. The spectrogram is the simplest nonlinear TF representation.

Since the spectrogram cannot produce ideal time and frequency concentration, other more sophisticated nonlinear representations have been proposed in the last 20 years. The Wigner distribution (WD) is the most commonly used of them defined as [23]:

$$WD_x(t,f) = \int_{-\infty}^{\infty} x(t+\tau/2)x^*(t-\tau/2)e^{-j2\pi f\tau}d\tau. \tag{7}$$

However, the WD exhibits significant drawbacks, since it produces the cross-terms for multicomponent signals. For example, for signal with two components $z(t) = x(t) + y(t)$ it follows:

$$WD_z(t,f) = WD_x(t,f) + WD_y(t,f) +$$

$$+2\,\mathrm{Re}\left\{\int_{-\infty}^{\infty} x(t+\tau/2)y^*(t-\tau/2)e^{-j2\pi f\tau}d\tau\right\}, \tag{8}$$

where the third component is undesired oscillatory cross-term between signal components. In the case of an M-component signal, number of cross-terms is $M(M-1)/2$. These cross-terms can be very emphatic and they can cover the useful TF components. Design of TF representations reducing or removing cross-terms is a difficult task [20].

Signals produced by nonlinear chaotic oscillators could have numerous components. Then we use the STFT (i.e., spectrogram) as the TF representation tool in order to avoid emphatic influence of cross-terms. Note that there are efficient hardware and software realizations of the STFT and spectrogram widely available in practice. Furthermore, since the STFT and spectrogram are time-varying forms of signal spectra, we can assume that all conclusions related to the FT and periodogram in various bifurcation regimes derived in [19] can be applied here.

III. Proposed detector

In order to present the background motivation for our detector of chaotic behavior, we consider the Chua's circuit with the following set of parameters: $L = 18$mH, $C_1 = 10$nF, $C_2 = 100$nF, $G_a = -757.576\mu$S, $G_b = -409.091\mu$S, $E = 1$V, $R_0 = 12.5\Omega$ with G in the range $G \geq 500\mu$S. Note that the global behavior of the circuit is analyzed in [19] for the same set of parameters. The varying conductance G given in Fig.2a is used as the bifurcation parameter. It produces so called period doubling route to chaos. This is the most widely observed and well-known route to chaotic behavior. Logarithm of the STFT magnitude for this route to chaos is visualized in the TF plane in Fig.3a[1]. The signal of interest is $v_1(t)$. Similar results are obtained for $v_2(t)$ and $i_3(t)$. The Hanning window of the width $T = 3$ms is used for evaluation of the STFT. For $t \in [0, 20\text{ms}]$, conductance is constant and equal to 530μS. The circuit exhibits a stable period 1 limit cycle in this interval. Signal in the TF plane in this interval (Fig.3a) has component that corresponds to main frequency at approximately 3kHz, higher harmonic components and DC component. For $t \in$ [20ms,100ms] the value of G linearly increases to 565μS. For $G = 537\mu$S a period-doubling or pitchfork bifurcation occurs. Then, a stable limit cycle eventually loses stability and now closes on itself after encircling an equilibrium point twice, which we shall refer to as a period 2 limit cycle. This periodic signal has a fundamental frequency component at approximately 1.5kHz (half of the main frequency component). Further increase of the conductance produces a cascade of period-doubling bifurcations to period 4, period 8, period 16, and so on, until an orbit of infinite period is reached, beyond which we have chaos. In the TF plane one can see numerous new components that appear at frequencies proportional to the main component frequency and at the multiples of the frequencies introduced by the bifurcation regime. In a chaotic regime only dominant frequency component can be easily seen, while other components appear to be covered with noise-like structures[2]. It has been shown [19] that the chaotic regime begins from $G = 541\mu$S (in our case it is for $t = 44$ms). This type of chaos is characterized by the spiral-Chua strange attractor given in Fig.2b. As the conductance G increases further, a double-scroll Chua strange attractor appears for $G = 552\mu$S. This kind of attractor is given in Fig.2c. Between the chaotic regions in the parameter space of Chua's circuit, there exist ranges of the bifurcation parameter G over which a stable periodic motion occurs. These regions of periodicity are called periodic windows. In our experiment after $t = 100$ms, G linearly decreases and circuit gradually returns from chaotic to periodic regime.

Logarithm of the STFT magnitude for some characteristic instants is given in the right part of Fig.3. For $t = 20.8$ms (Fig.3e) the circuit is in a period 1 stable orbit. Dominant spectral components (DC and main sinusoidal component) and higher harmonics can

[1]Logarithm of the STFT magnitude is used hereafter for visualization, in order to present numerous weak signal components.

[2]These structures are in fact sum of infinite number of sinusoidal components with frequencies equal to multiple of the fractions of the main frequency component in a stable state.

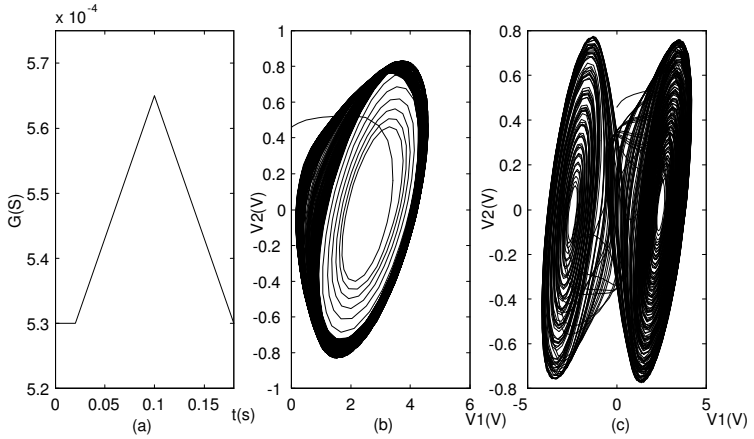

Fig. 2. (a) The varying conductance G; (b) Spiral Chua strange attractor $G = 541\mu$S; (c) Double scroll Chua strange attractor $G = 552\mu$S.

be observed. For $t = 39.8$ms the circuit is in a region of cascade period doubling oscillations and numerous peaks can be seen in the spectral domain (Fig.3d). The subharmonic $f = 1.5$kHz is excited (period 2 motion), and the spectrum contains peaks at frequencies corresponding to a linear combination of the subharmonic and main frequency. It can be noticed that all "new" spectral peaks are small compared to the DC and main spectral component. Therefore, components caused by period doubling bifurcations are sinusoids in the region above the main spectral component and between the DC and main spectral component. For $t = 57.8$ms the circuit is in a chaotic regime. The DC and the main frequency component peaks are no longer dominant as in the previous two cases (see Fig.3c). Especially, it is important to note that spectral content in the area between two dominant peaks is increased and of the same order of magnitude as the dominant components. The TF representation for the instant within periodic window is shown in Fig.3b. The spectral content is similar to the stable orbit case (see Fig.3e).

From this experiment we conclude that the spectral content of signal between the DC and the main spectral component could be used as a detector of chaotic state. The first step in chaos detection is frequency estimation of the main spectral component. In the region of periodic signal, frequency can be estimated in a simple manner as a position of the maximum in the STFT, excluding region around the DC component:

$$f_m(t) = \arg\max_{f>\varphi} |STFT(t, f)|, \qquad (9)$$

where φ is the region of DC component that is only several frequency samples wide (details are given later in this section). However, it cannot be done in the same manner if DC and main spectral components are very close to each other. Then, a more precise technique such as ESPRIT (Estimation of Signal Parameters via Rotational Invariance Techniques) should be employed [24]. Since the ESPRIT and other similar techniques could be sensitive to additive noise, estimation of the dominant component is performed in two stages. In the first one, dominant frequency component is estimated by both procedures. The ESPRIT algorithm output is taken as a more precise frequency estimate if both procedures produce similar results. However, if the results significantly differ, frequency estimate from the previous instant is used, assuming that the main spectral component cannot vary significantly in a narrow interval. Note that in our experiments, the frequency of the main component is not calculated in each instant, but only in the equidistantly spaced intervals.

In the next step, current circuit state is estimated based on the spectral content between DC and the main spectral component. Chaotic

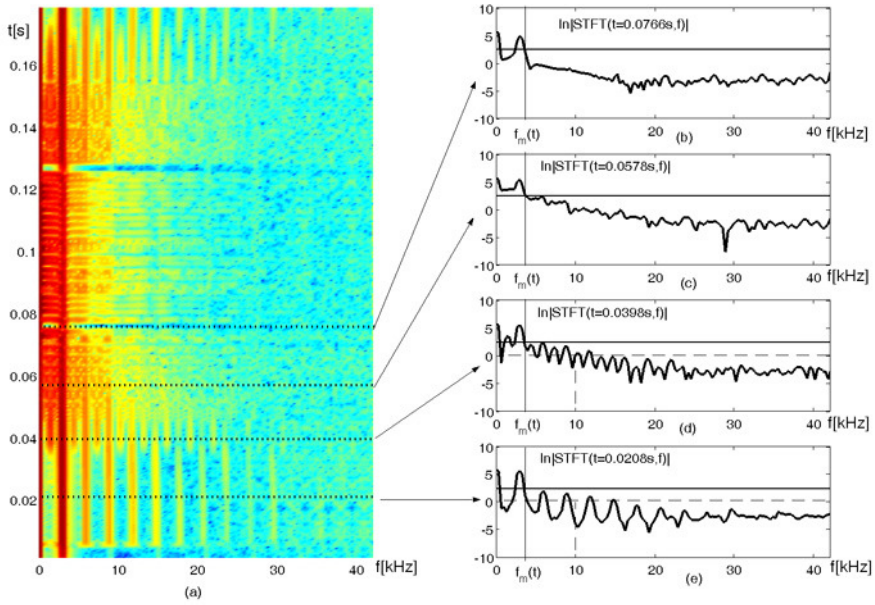

Fig. 3. Period doubling route to chaos: (a) STFT; (b) logarithm of the STFT for $t = 76.8$ms - periodic window; (c) logarithm of the STFT for $t = 57.8$ms - chaos; (d) logarithm of the STFT for $t = 39.8$ms - period doubling interval; (e) logarithm of the STFT for $t = 20.8$ms - period 1 orbit.

behavior measure is defined as:

$$m(t) = \int_0^{f_m(t)} u_{\Omega(t)}(t; f)df, \tag{10}$$

where the function $u_{\Omega(t)}(t; f)$ is given as

$$u_{\Omega(t)}(t; f) = \begin{cases} 1 & |STFT(t, f)| \geq \Omega(t) \\ 0 & \text{elsewhere.} \end{cases} \tag{11}$$

Parameter $\Omega(t)$ is selected in such a way that the STFT values with magnitude higher than $\Omega(t)$ contain almost all signal energy, i.e., the energy that remains outside this region is very small:

$$(1 - \varepsilon) \int_0^{\infty} |STFT(t, f)|^2 df =$$

$$= \int_0^{\infty} |STFT(t, f)|^2 u_{\Omega(t)}(t; f)df. \tag{12}$$

In our experiments $\varepsilon = 0.0025$ is selected, i.e., 99.75% of the signal energy within the considered window is contained in the region producing values larger than $\Omega(t)$. Note that our algorithm works well for relatively wide range of parameter ε. Selection of $\Omega(t)$ can be performed in a simple manner. The magnitudes of STFT samples in the considered instant are sorted into decreasing order and $\Omega(t)$ is selected as a position where the remaining part of the sorted sequence has energy less or equal to $\varepsilon \int_0^{\infty} |STFT(t, f)|^2 df$. For the presented example in Fig.3b-e, $\Omega(t)$ is given as a solid horizontal line.

Proposed chaos detector $m(t)$ measures the region between DC and the main spectral component with relatively high energy. In the periodic regime $m(t)$ is relatively small, equal to width of the DC and main spectral components, while in the chaotic region it would be higher due to additional components.

Note that, in order to avoid possible influence of noise and other errors, the obtained detector response $m(t)$ is averaged within short interval around the considered instant:

$$m'(t) = \frac{1}{p} \int_{t-p/2}^{t+p/2} m(\tau)d\tau. \tag{13}$$

Based on $m'(t)$, we take the following decision:

$$\begin{array}{ll} m'(t) \geq C(t) & \text{chaotic regime} \\ m'(t) < C(t) & \text{periodic regime.} \end{array} \quad (14)$$

Detection threshold $C(t)$ can be determined as follows. In the chaotic regime, it is expected that the spectrogram in the entire region $[0, f_m(t)]$ is above the detection threshold. In that case, the expected value of $m'(t)$ in the chaotic regime is close to $f_m(t)$. However, in the periodic regime (or in the part of period doubling) values of the STFT between the DC and main spectral component are small. We can assume that the width of signal components is known and determined by the used window function. In the case of discretized signal used in numerical calculation, application of the Hanning window produces three nonzero frequency samples. We assumed that expected value of $m'(t)$ in periodic regimes, for the Hanning window of the width T, is equal to 5 frequency samples $(5/T)$: 3 of the main component and 2 of the DC component. Note that one sample of the DC component is in the negative frequency region. The detection threshold is selected as the arithmetic mean between expected values of detector response in periodic and chaotic regimes:

$$C(t) = \frac{f_m(t) + \frac{5}{T}}{2}. \quad (15)$$

The algorithm is summarized in Table I. Note that detector response ($m(t)$ or $m'(t)$) as well as detector threshold $C(t)$ are measured in Hz.

Comments on the algorithm. 1. The most important point in the algorithm is selection of ε. If ε is selected to be too small, detector response function would estimate entire interval as a chaotic state. However, the TF representation samples between the DC and the main signal component are at least an order of magnitude larger in chaotic than in the periodic regime. It provides a safe margin for selection of the current state in the circuit.

2. Region of period doubling intervals can be more challenging for estimation. For period 2, period 4 and period 8 orbits the same procedure can be performed. After detection of chaotic regime, $\Omega(t)$ can be decreased for an order of magnitude, while frequency range, over which detector is calculated, should be increased (for example given in Fig.3d, frequency region for evaluation of the second measure can be enlarged up to 10kHz). In the case of stable orbit regime (including periodic windows) expected value of $m'(t)$ is increased for the width of one or two spectral components, comparing to the case when evaluation is performed over the interval $[0, f_m(t)]$. However, in the period doubling region it will be increased several times, since numerous additional sinusoidal components will be detected. This value is depicted with dashed lines in Figs.3c and 3d. In both cases, the first detection step would detect whether a signal is in periodic or period doubling interval. The period doubling behavior would be detected in the second step. Note that period 16 and other "higher order" orbits cannot be detected by this procedure, and they will be detected as chaotic regime. This is not a serious drawback, since such periodic orbits have similarities with chaotic behavior.

3. Decision to adopt this kind of procedure has been made after several attempts to estimate behavior of the circuit based on some classical TF concentration measures [25],[26] failed to produce accurate results. There are several reasons for this, but the main point is in a very complicated structure of signal with numerous sinusoidal components different in magnitude and with noise like structures. Common concentration measures exhibit similar concentration for noise interval and for interval with numerous harmonic components that may appear in the period doubling bifurcations. Therefore, they cannot be used to distinguish between these regions.

In the next section, application of the proposed estimator is considered in the case of several common routes to chaos. Also, analysis of the proposed algorithm in the case of signals corrupted by noise is given.

IV. Simulation study

In this section, we consider detector response in the case of various routes to chaos. Firstly, we present the results obtained in the

TABLE I
SUMMARY OF THE ALGORITHM FOR CHAOTIC BEHAVIOR DETECTION.

Step 1.	**Calculation of the STFT by using (5).**
Step 2.	**Dominant spectral component frequency estimation.** **2a.** Position of the TF representation maximum is adopted as a dominan frequency in initial instant $t = t_0$. **2b.** For the next instants, frequency of the main spectral component $f_m(t)$ is estimated by using the ESPRIT, $f'_m(t)$, and position of the maximum (9), $f''_m(t)$, respectively. **2c.** Result from the ESPRIT algorithm is used as a frequency of dominant spectral component if $\lvert f'_m(t) - f''_m(t)\rvert \leq \rho$, where $\rho = 2/T$ (two frequency samples). Otherwise, we selected value the that is closer to the frequency estimated for the previous instant: $f_m(t) = \begin{cases} f'_m(t) & \text{for } \lvert f'_m(t) - f_m(t-1)\rvert < \lvert f''_m(t) - f_m(t-1)\rvert \\ f''_m(t) & \text{otherwise.} \end{cases}$
Step 3.	**Determination of** $\Omega(t)$. **3a.** Sort the STFT samples in order to obtain the sequence decreasing in magnitude. **3b.** Parameter $\Omega(t)$ is selected as a value of the STFT such that the remaining (smaller) samples of the STFT in the considered instant produce energy less than $\varepsilon \int_0^\infty \lvert STFT(t,f)\rvert^2 df$.
Step 4.	**Calculation of detector response function.** **4a.** Calculation of $m(t)$ using (10). **4b.** Averaging in the local neighborhood, (13). In our experiments local neighborhood is 5% of the used window.
Step 5.	**Determination of current state by** (14)**.**

case of the period doubling route to chaos (already used in previous simulation) in Section IV.A. Then two other routes, torus breakdown and intermittency routes, are analyzed in Sections IV.B and IV.C. In order to show that application of the proposed detector is not limited to the chaotic oscillatory circuits, well-known Rossler and logistic map chaotic systems are analyzed in Sections IV.D and IV.E. Detector accuracy in the noise environment is studied for a signal produced by the Chua's circuit transmitted through the communication lines, Section IV.F.

A. Period doubling route to chaos

In this example we applied the previously used setup (see Section III) to illustrate detector accuracy for period doubling route to chaos. Illustration of the TF representation is repeated in Fig.4a, while the detector response function is given in Fig.4b. Dotted box represents the region with chaotic behavior according to [19]. It can be seen that region where the proposed detector response is above the threshold well corresponds to the theoretical expectations. Also, two periodic windows are properly detected.

B. Torus breakdown route to chaos

The second considered route to chaos is quasiperiodic or torus breakdown route. It is the oldest introduced route to chaos, but it still remains to be thoroughly studied. This type of bifurcations could be detected in numerous types of real physical systems [27]. In this route to chaos, a torus attractor bifurcates into periodic orbits of consecutively decreasing periods, i.e., windows of quasiperiodic and periodic behavior alternate by varying a parameter. In the torus breakdown route to chaos

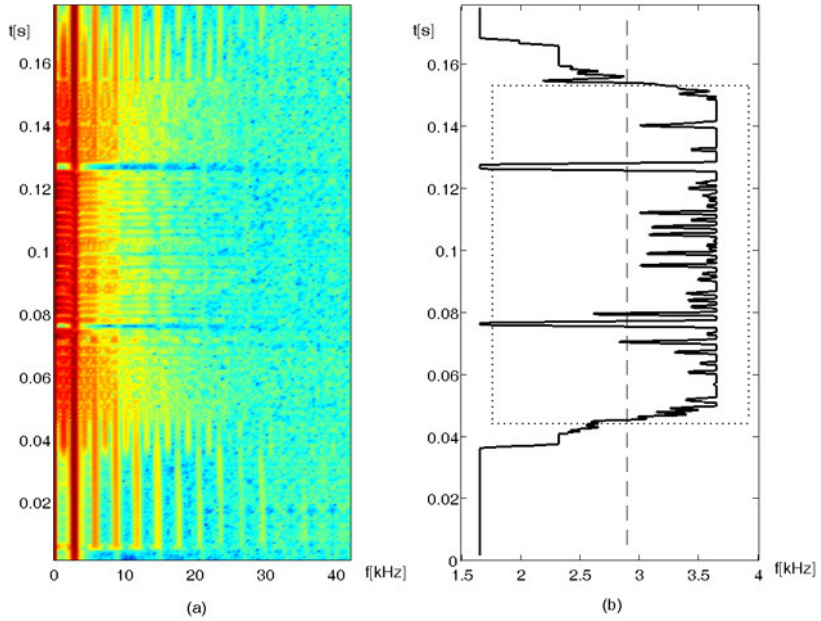

Fig. 4. Period doubling route to chaos: (a) time-frequency representation; (b) thick line - detector response; dotted box - region of chaos according to theoretical assumptions; dash line - threshold.

system undergoes several Andronov-Hopf bifurcations and after that a periodic orbit finally bifurcates into chaotic attractor through a period-doubling sequence. In order to consider a torus breakdown route to chaos in the Chua's circuit, the parameters: $L = 7.682$mH, $C_2 = 0.3606\mu$F, $G_a = 0.599$mS, $G_b = 0.77$mS, $E = 1$V, $R_0 = 13.4\Omega$, $G = -0.7$mS are fixed [28]. The varying parameter was C_1. It linearly decreases from $C_1 = 0.0297\mu$F to $C_1 = 0.008\mu$F, and after that increases toward the initial value. This route to chaos is visualized in Fig.5 with the TF representation on the left hand side and the corresponding detector response given on the right hand side. The steady-state trajectory for $C_1 = 0.0297\mu$F is a torus, and two incommensurate frequencies can be observed in the spectrum. During the decrease of C_1 from $C_1 = 0.02\mu$F ($t = 0.035$s) to $C_1 = 0.0157\mu F$ ($t = 0.05$s), sequence of periodic windows of decreasing periods is produced. The torus attractors can be observed between the periodic windows. If parameter C_1 is further decreased to $C_1 = 0.0127\mu$F ($t = 0.062$s), a period-doubling sequence ending in a chaotic attractor is obtained. Numerous new frequency components can be seen in the TF plane. Dotted line in Fig.5b depicts approximative region of the chaotic behavior based on theoretical consideration [28]. It can be seen that this region corresponds well with the obtained region where detector response is above the threshold.

C. Intermittency route to chaos

The third route to chaos is the Manneville-Pomeau intermittency route [29]. Intermittency is the phenomenon where the signal is virtually periodic, except for some irregular (unpredictable) bursts. In other words, there are intermittently periodic and irregular aperiodic behavior. The dynamic system has a periodic orbit over a certain range of a varying parameter. When the parameter is tuned beyond a critical value, some irregular short bursts appear among the long regular intervals. With further changes of the parameter, the bursts appear more frequently and the

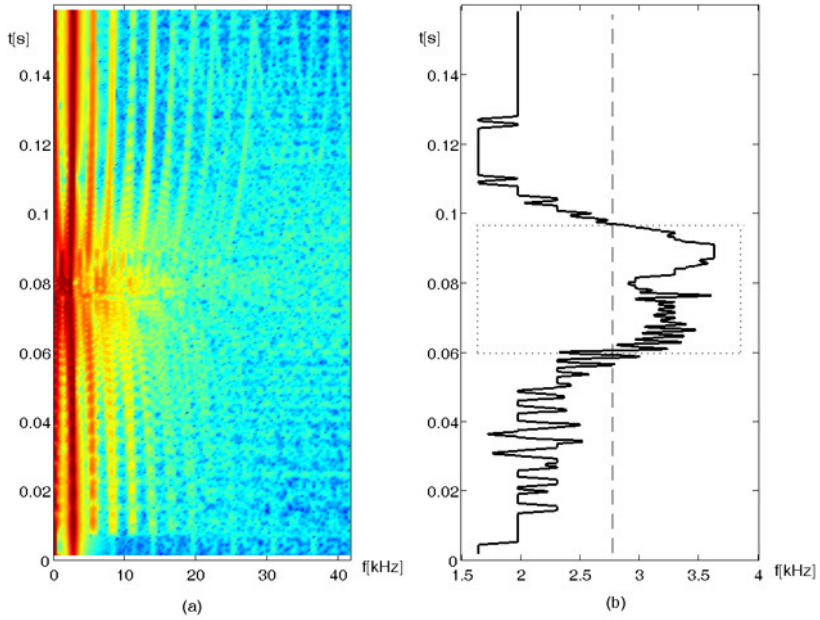

Fig. 5. Torus breakdown route to chaos: (a) logarithm of the $|STFT(t,\omega)|$; (b) detector response - thick solid line; detection threshold - dashed line; chaotic region defined by theory - dotted line.

average time between two consecutive bursts shortens. Eventually, the system moves into a chaotic regime. The phenomenon associated with this route is a saddle-node bifurcation, which qualitatively differs from other two routes.

In our experiment parameters $G_a = -0.756$mS, $G_b = -0.409$mS, $E = 1$V, $L = 37.56$mH, $C_2 = 215$nF, $R_0 = 30\Omega$, $G = 0.648$mS are constant [30]. Parameter C_1 linearly varies from $C_1 = 19.28$nF to $C_1 = 19.246$nF. With decreasing of C_1, periodical windows become narrower.

The STFT of the signal obtained for this route to chaos is given in Fig.6, left column, while the corresponding detector response is given in the right column. Detection threshold is depicted with dashed vertical line. In this case, frequency of the main spectral component is calculated every 200ms. The main frequency is 0.32kHz in the interval $0 \leq t \leq 1$s and 0.25kHz in the interval $1 < t \leq 1.6$s. Consequently, in these two regions, the threshold is different (dashed line in Fig.6b). In the periodic regime the detector response function is small, below the threshold, since detector counts only samples belonging to sinusoidal components. However, in the chaotic regime, due to the additional components, detector response function is higher than the detection threshold. Note that all visible periodic windows are detected.

D. Rossler attractor

In order to show that this detector can be applied to other chaotic systems, we consider the well known Rossler [31] and logistic map [14] chaotic systems. The Rossler system can be described with three differential equations:

$$\begin{aligned} \frac{dx}{dt} &= -y - z \\ \frac{dy}{dt} &= x + ay \\ \frac{dz}{dt} &= b + z\,(x - c)\,. \end{aligned} \tag{16}$$

In our simulations we set $a = b = 0.2$ while parameter c increases from 2 to 5.7 within

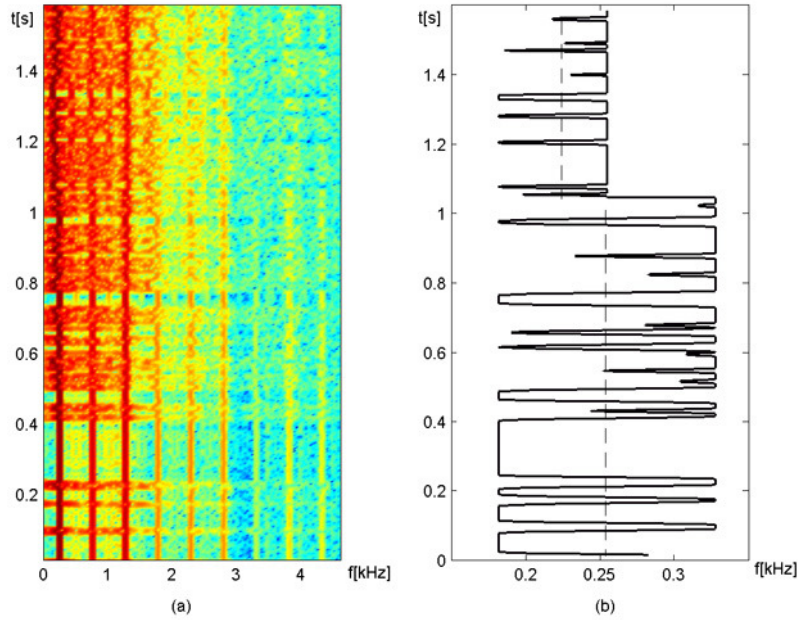

Fig. 6. Intermittency route to chaos: (a) logarithm of $|STFT(t,\omega)|$; (b) detector response - thick solid line; detection threshold - dashed line.

$0 < t < 1500$s [31]. After period 1 limit cycle ($0 < t < 600$s) the system undergoes a period-doubling bifurcation ($t = 600$s, $c = 3.26$). Further increase of c produces a period-doubling sequence while chaotic attractor appears for $c = 4.31$. In our experiment after $t = 1500$s, parameter c linearly decreases and system returns to periodic regime. This route to chaos is visualized for signal $x(t)$ in Fig.7 with the TF representation on the left hand side and the corresponding detector response given on the right hand side. Region in the dotted box is chaotic according to theoretical consideration from [31]. The proposed detector produces accurate results close to the theoretical ones.

E. Logistic map

The logistic map is one of the simplest known chaotic systems given by difference equation:

$$x_{n+1} = Ax_n\left(1 - x_n\right). \tag{17}$$

Even this very simple form, with single variable and control parameter A, could produce chaotic behavior like more complicated chaotic systems. This system is used to model numerous phenomena in practice [14].

In our experiment, parameter A is linearly varied in the range from 3.5 to 4. Initial condition is $x_0 = 0.1$. For $A = 3.57(n = 2200)$ the accumulating point has been reached and after that instant we have the chaotic regime. However, in chaotic regime there are infinitely many periodic windows [14]. The proposed method accurately detected chaotic regime and three relatively long periodic windows (see TF representation in Fig.8a). Detector response is given in Fig.8b.

F. Noise influence

It order to analyze robustness of the proposed detector to noise influence, it was assumed that the signal produced by the Chua's circuit is transmitted through a noise channel. Noise environment was Gaussian. We varied signal to noise ratio (SNR) within $SNR \in$

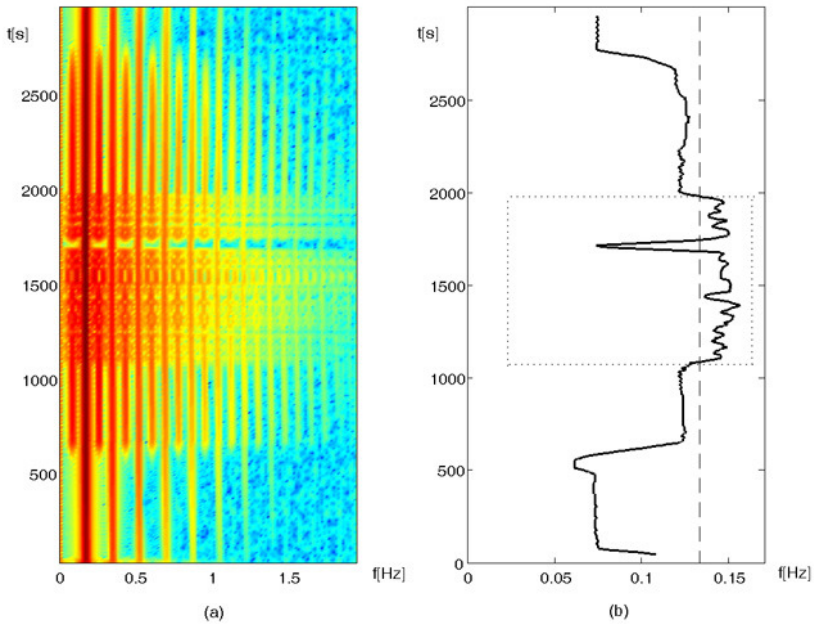

Fig. 7. Period doubling route to chaos for Rossler system: (a) TF representation; (b) thick line - detector response; dotted box - region of chaos according to theoretical analysis; dash line - detection threshold.

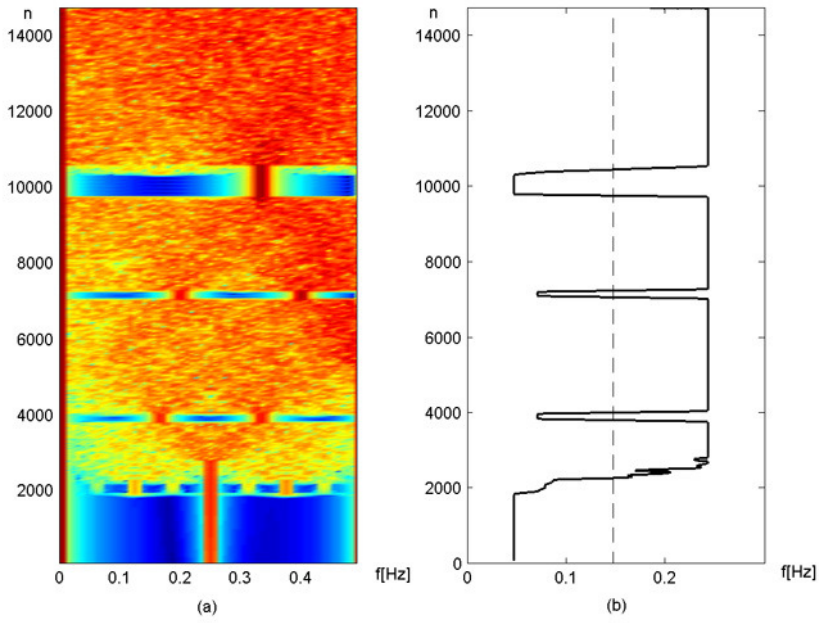

Fig. 8. Period doubling route to chaos for logistic map: (a) TF representation; (b) thick line - detector response, dashed line - threshold.

[8, 20]dB. The SNR is evaluated as:

$$SNR = 10\log_{10}\frac{\int\limits_t |f(t)-\overline{f}(t)|^2 dt}{\int\limits_t |\nu(t)|^2 dt} \qquad (18)$$

where $\overline{f}(t)$ is the signal mean value in the short interval around considered instant:

$$\overline{f}(t) = \frac{1}{T}\int\limits_{t-T/2}^{t+T/2} f(\tau)d\tau. \qquad (19)$$

Parameter T is equal to the used window width in the STFT ($T = 3$ms)[3]. Detector response for two various SNRs in the period doubling route to chaos is depicted in Fig.9. Experiment setup is changed with respect to Section IV.A, in order to have more periodic windows within interval of interest. For $SNR = 20$dB the detector finds 4 windows denoted by w_i, $i = 1, ..., 4$ in Fig.9a. However, the detector for $SNR = 10$dB detects all of them, but with windows w_2 and w_3 eroded comparing to the previous case, Fig.9b. These two windows will not be detected for lower SNR values. Accuracy of the proposed detector is tested in the Monte-Carlo simulation in 100 trials. As an accuracy measure, percentage of periodic regime samples recognized as chaotic samples (A) and of percentage periodic window samples detected as chaos (B) are selected. Results are summarized in Table II. Percentage of misidentified samples of the periodic regime is small even for relatively high noise of $SNR = 10$dB. It cannot be said for narrow periodic windows. Namely, the STFT evaluated for an instant within narrow periodic window is calculated by using samples from both periodic window and neighbor chaotic region. For noisy environment it causes that samples close to the borders of the periodic window are misidentified as a chaotic signal. Since the chaotic regime is detected as a region with noise-like structures, detected chaotic region is enlarged for signals corrupted by significant amount of Gaussian noise.

[3]The SNR definition is in accordance with Donoho's paper [32].

TABLE II
PERCENTAGE OF DETECTION ERRORS FOR SIGNAL CORRUPTED BY GAUSSIAN NOISE FOR PERIOD DOUBLING ROUTE TO CHAOS. A - ERRORS IN PERIODIC REGIME; B - ERRORS WITHIN PERIODIC WINDOWS.

SNR	A	B
20dB	0.4%	4.70%
17dB	0.95%	6.31%
14dB	2.04%	9.51%
12dB	3.37%	17.74%
10dB	5.98%	38.09%
8dB	23.68%	61.51%

V. BREAKING CHAOTIC COMMUNICATIONS

Chaotic shift keying or chaotic switching is a method of chaos-based secure communications. In this method, a binary information signal is encoded into two sets of parameters of the chaotic transmitter, i.e., two different chaotic attractors. These two chaotic attractors have almost the same shapes and statistical properties in the phase space. Standard approach to recover binary signal from transmitted signal $v_1(t)$ at the receiver is by using the synchronization error.

However, this kind of secure communication scheme has its drawbacks [21], [33]-[35]. An alternative method for breaking secure communication scheme is considered here. It uses the detector response function for breaking secure communications based on the Chua's circuit signal. In our simulations, we use the same parameter sets as in [21]: $G = 1$mS, $G_a = -1.139$mS, $G_b = -0.711$mS, $E = 1$V, $R_0 = 20\Omega$ are fixed, while binary digit 1 is encoded with $L = 12$mH, $C_1 = 17$nF and $C_2 = 178$nF (first parameter set), binary digit 0 is encoded with $L = 12.4$mH, $C_1 = 17.5$nF, $C_2 = 195$nF (second parameter set). In both cases, the system produces different, but qualitatively similar, Rossler-like attractors. Information bearing signal, bin(t), is given in Fig.10a, while transmitted signal $v_1(t)$ is given in Fig.10b.

Instead of using the Chua's circuit at the receiver side, we applied the proposed TF representation based detector. Fig.11a depicts STFT of the signal $v_1(t)$. It is hard to ob-

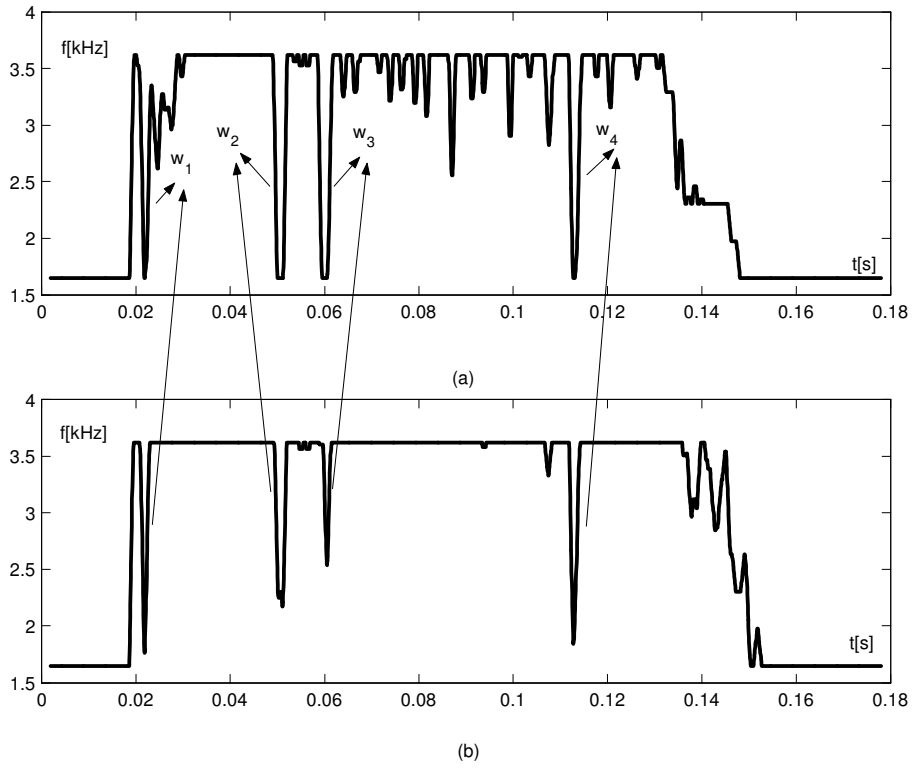

Fig. 9. Detector response for: (a) $SNR = 20$dB; (b) $SNR = 10$dB.

serve any difference between STFT of different signals. However, there is a difference in concentration of the TF distribution for signals of different attractors. This difference can be detected and used as a base for reconstructing binary message. Detector response is determined according to the proposed algorithm (Table I, Step 1 to Step 4). The difference in STFT's concentration for different chaotic attractors is obvious (Fig.11b). For comparison, the message signal is plotted in the same figure. The response of the proposed detector could be mapped to binary form by using a suitable threshold.

The proposed breaking scheme has been tested for additive Gaussian noise environment with $SNR \in [8, 40]$dB. Detector threshold is $C(t) = 4.67$kHz. The percentage of misidentified samples has been considered as accuracy measure and it is given in Fig.12. Note that one bit of information has width of approximately 160 samples. In our experiments we reconstructed accurately all bits of information for percentage of misidentified samples less than 10%, i.e., for $SNR > 12$dB.

The proposed detector can also be used for breaking chaotic communications produced by hyperchaotic systems [21] but with reviewed detector setup (higher parameter ε in (12)). This research will be reported elsewhere.

VI. Conclusion

A simple detector of chaotic behavior is presented. The time-varying behavior of the chaotic nonlinear oscillators is investigated by using the concentration measure of the STFT samples. The proposed method has been shown to be very accurate for different routes to chaos and various chaotic systems. Furthermore, it can be used in moderate noise environments to distinguish between the chaos and noise influenced samples. This is an important feature, since there are numerous similarities between the chaotic and noise signals. The

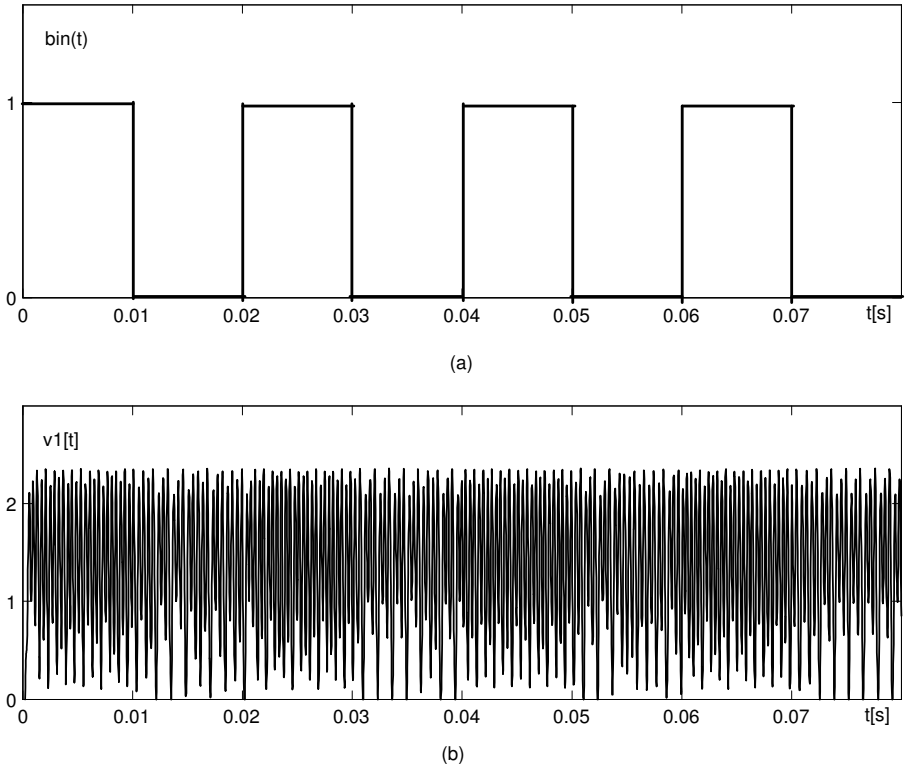

Fig. 10. (a) The binary message $\mathrm{bin}(t)$; (b) The transmitted signal $v_1(t)$.

proposed method can track very small differences in the chaotic attractors and it can be applied for breaking chaotic communications. Numerical analysis is presented in the case of the Chua's circuit, and some other well known chaotic systems. The proposed approach is tested on other kinds of chaotic oscillators, and obtained results are accurate. In future research, we will try to improve the proposed estimator in order to be able to track more complicated features of the chaos, i.e., to distinguish between various attractors.

VII. Acknowledgement

The authors are very thankful to the reviewers for insights that helped us to improve the paper. The authors are thankful to Prof. Z. Uskoković for numerous helpful comments and proof reading of the revised version of the paper.

References

[1] M. P. Kennedy, "Chaos in the Colpitts oscillator," *IEEE Trans. Circ. Syst. I*, vol. 41, no. 11, pp. 771-774, Nov. 1994.

[2] A. L. Baranovski and W. Schwarz, "Chaotic and random point processes: Analysis, design, and applications to switching systems," *IEEE Trans. Circ. Syst. I*, vol. 50, no. 8, pp. 1081-1089, Aug. 2003.

[3] K. M. Cuomo, A. V. Oppenheim and S. H. Strogatz, "Synchronization of Lorenz-based chaotic circuits with applications to communications," *IEEE Trans. Circ. Syst. II*, vol. 40, no. 10, pp. 626-632, Oct. 1993.

[4] N. J. Corron and D. W. Hahs, "A new approach to communications using chaotic signals," *IEEE Trans. Circ. Syst. I*, vol. 44, no. 5, pp. 373-382, May 1997.

[5] A. Tefas, A. Nikolaidis, N. Nikolaidis, V. Solachidis, S. Tsekeridou and I. Pitas, "Markov chaotic sequences for correlation based watermarking schemes," *Chaos, Solutions and Fractals,* vol. 17, no. 2, pp. 567-573, July 2003.

[6] W. A. Brock, D. A. Hsieh and B. LeBaron, *Nonlinear dynamics, chaos, and instability: statistical theory and economic evidence*, MIT Press, Cambridge, MA, 1991.

[7] D. Mackey and L. Glass, "Oscillation and chaos in physiological control systems," *Science*, vol. 197,

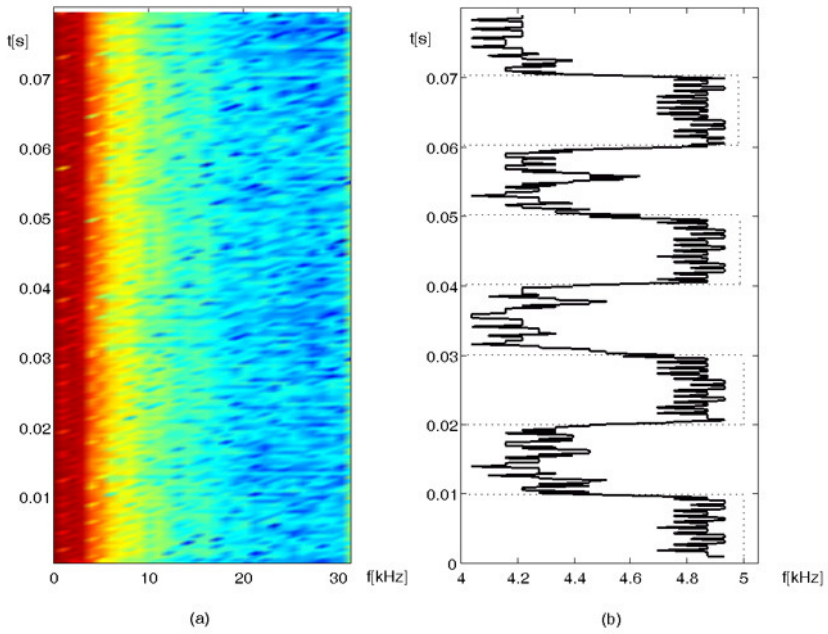

Fig. 11. Breaking chaotic communications: (a) STFT of the transmitted signal $v_1(t)$; (b) Detector response; binary message-dotted line.

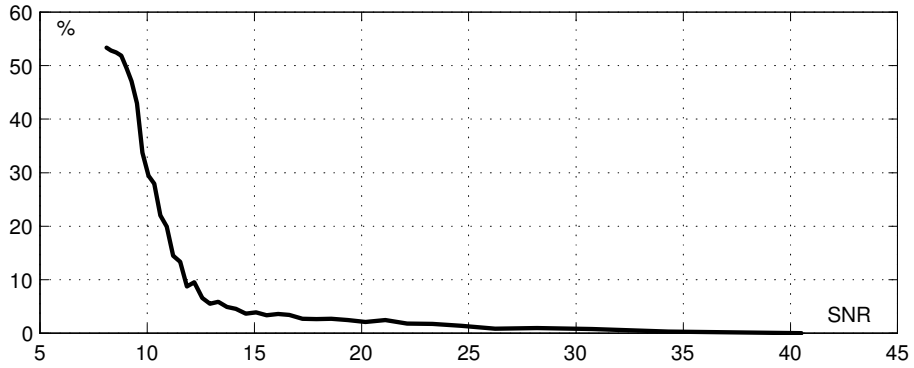

Fig. 12. Percentage of misidentified samples in breaking chaotic secure communications.

pp. 287-289, July 1977.

[8] Y. Nakamura and A. Sekiguchi, "The chaotic mobile robot," *IEEE Trans. Robotics and Automation,* vol. 17, no. 6, pp. 898-904, Dec. 2001.

[9] C.-S. Poon and M. Barahona: "Titration of chaos with added noise," *Proc. of NAS*, vol. 98, no. 13, 2001, pp. 7107-7112.

[10] P. Drazin: *Nonlinear systems*, Cambridge Univ. Press, 1992.

[11] M. Palus and D. Novotna: "Sunspot cycle: A driven nonlinear oscillator," *Phys. Rev. Lett.*, vol. 83, no. 17, 1999, pp. 3406-3409.

[12] A. Wolf, J. B. Swift, H. L. Swinney, and J. A. Vastano, "Determining Lyapunov exponents from a time series," *Physica D*, vol. 16, 1985, pp. 285-317.

[13] M. R. Rosenstein, J. J. Collins, C. J. De Luca, "A practical method for calculating largest Lyapunov exponents for small data sets," *Physica D*, vol. 65, 1993, pp. 117-134.

[14] J. C. Sprott, *Chaos and Time-Series Analysis*, New York: Oxford University Press, 2003.

[15] T. S. Parker and L. O. Chua, "Chaos: A tutorial for engineers," *Proc. IEEE*, vol. 75, no. 8, pp. 982-1007, Aug. 1987.

[16] H. D. I. Abarbanel, T. W. Frison and L. S. Tsirm-

ing, "Obtaining order in a world of chaos," *IEEE Signal Proc. Magaz.*, vol. 15, no. 3, pp. 49-65, May 1998.

[17] G. Sugihara and R. M. May: "Nonlinear forecasting as a way of distinguishing chaos from measurement error in time series," *Nature*, no. 344, 1990, pp. 734-741.

[18] T. Schreiber: "Constrained randomization of time series data," *Phys. Rev. Lett.*, vol. 80, pp. 2105–2108, 1998.

[19] M. P. Kennedy, "Three steps to chaos-Part II: A Chua's circuit primer," *IEEE Trans. Circ. Syst.*, vol. 40, no. 10, pp. 657-674, Oct. 1993.

[20] B. Boashash, ed: *Time-frequency signal analysis and applications*, Elsevier, 2003.

[21] T. Yang, L. B. Yang and C. M. Yang, "Breaking chaotic secure communication using a spectrogram," *Phys. Lett. A,* vol. 247, no. 1-2, pp. 105-111, Oct. 1998.

[22] J. B. Allen and L. R. Rabiner, "A unified approach to short-time Fourier analysis and synthesis," *Proc. IEEE*, vol. 65, no. 11, pp. 1558-1564, Nov. 1977.

[23] L. Cohen, "Time-frequency distributions-a review," *Proc. IEEE*, vol. 77, no. 7, pp. 941-981, July 1989.

[24] P. Stoica and R. L. Moses, *Introduction to spectral analysis*, Prentice-Hall, 1997.

[25] R. G. Baraniuk, P. Flandrin, A. J. E. M. Janssen and O. J. J. Michel, "Measuring time-frequency information content using the Renyi Entropies," *IEEE Trans. Inf. Th.*, vol. 47, no. 4, pp. 1391-1409, May 2001.

[26] LJ. Stanković, "A measure of some time-frequency distributions concentration," *Sig. Proc.*, vol. 81, no. 3, pp. 621-631, Mar. 2001.

[27] T. Matsumoto, L. O. Chua and R. Tokunaga, "Chaos via torus breakdown," *IEEE Trans. Circ. Syst.*, vol. 34, no. 3, pp. 240-253, Mar. 1987.

[28] L. O. Chua, C. W. Wu, A. Huang and G. Q. Zhong, "A universal circuit for studying and generating chaos-Part I: Routes to chaos," *IEEE Trans.Circ. Syst.*, vol. 40, no. 10, pp. 732-744, Oct. 1993.

[29] L. O. Chua and G. Lin, "Intermittency in a piecewise-linear circuit," *IEEE Trans. Circ. Syst.*, vol. 38, no. 5, May 1991.

[30] C. W. Wu, "Studying chaos via 1-D maps-A tutorial," *IEEE Trans. Circ. Syst.*, vol. 40, no. 10, pp. 707-721, Oct.1993.

[31] O. E. Rossler, "An equation for continuous chaos," *Phys. Lett. A*, vol. 57*,* pp. 397-398, 1976.

[32] D. L. Donoho and I. M. Johnstone, "Adapting to unknown smoothness via wavelet shrinkage," *JASA*, vol. 90, no. 432, pp. 1200-1224. 1995.

[33] T. Yang, "Recovery of digital signal from chaotic switching," *Int. J. Circuit Theory Appl.*, vol. 23, no. 6, pp. 611-615, Nov.-Dec. 1995.

[34] T. Yang, L. B. Yang and C. M. Yang, "Cryptanalyzing chaotic secure communications using return maps," *Phys. Lett. A,* vol. 245, no. 6, pp. 495-510, Aug. 1998.

[35] T. Yang, L. B. Yang and C. M. Yang, "Breaking chaotic switching using generalized synchronization: Examples," *IEEE Trans. Circ. Syst.*, vol. 45, no. 10, pp. 1062-1067, Oct. 1998.